

Recent Advances in Retinal Imaging With Adaptive Optics

Joseph Carroll, Daniel C. Gray, Austin Roorda and David R. Williams

Since its first application to retinal imaging nearly a decade ago, adaptive optics has helped researchers make fundamental advances in the understanding of how the human visual system works. The authors review these advances and describe what the future of adaptive optics in retinal imaging may hold in store.

Adaptive optics imaging systems use active optical elements to compensate for aberrations in the optical path between the camera and the object being imaged. In 1953, Babcock first suggested the use of adaptive optics to improve ground-based astronomy, where the rapidly changing atmosphere can significantly degrade the image quality of a ground-based telescope system.¹ Of course the use of adaptive optics is not limited to astronomical imaging, and in the past few decades there has been a rapid expansion in the applications for which adaptive optics has proven valuable.² In vivo medical imaging devices often image tissue through intervening aberrated media, which, like the turbulent atmosphere in the case of ground-based telescope systems, degrades the

image. In vitro light microscopy is hampered by specimen-induced aberrations; correcting these aberrations (optically or computationally) with adaptive optics results in increased axial resolution and signal intensity.^{3,4} Surgical procedures also stand to benefit from adaptive optics, since the delivery of laser power during retinal and endoscopic surgeries is limited by aberrations induced by the intervening media. Long-range laser communication is made possible by use of adaptive optics to reduce atmospheric aberrations.

An especially promising application of adaptive optics is the imaging of the living retina at high resolution. Vision scientists and ophthalmologists have long been interested in imaging cellular structures in the living retina to examine

photoreceptor properties in vivo and to more precisely characterize retinal disease. But the human eye suffers from higher order aberrations (induced mainly by the lens and cornea) that degrade retinal image quality and limit spatial vision. In 1961, Smirnov was the first to suggest the correction of these higher order aberrations to improve the optical performance of the eye.⁵ There was some initial success in recovering the spatial properties of the cone mosaic with speckle interferometry,⁶ which largely bypasses these aberrations. That same year, Dreher et al. were the first to use a deformable mirror to improve the quality of retinal images, though they only corrected the astigmatism of the eye (a lower order aberration) based on a subjective refraction.⁷ Correcting only lower order

aberrations, Miller et al. obtained the first direct images of single cells in the living human eye with high-magnification fundus imaging.⁸

A limitation of these earlier approaches was the inability to accurately and rapidly characterize the eye's higher order aberrations. To overcome this, Liang et al.⁹ developed a wavefront sensor for the eye that was subsequently improved to the point at which aberrations could be measured up to the 10th order.¹⁰ This enabled the use of adaptive optics to correct multiple higher order aberrations simultaneously, yielding substantially higher-resolution images than had previously been possible.¹¹ Further improvements in the wavefront sensor allowed real time measurement of the eye's wave aberrations and opened the door for future "closed-loop" systems.^{12, 13} Since the initial work of Liang and colleagues, high-resolution retinal imaging has found a home in vision science, where it is used by a number of researchers to further our understanding of the human retina. The goal of this article is to review the scientific advances made possible with adaptive optics retinal imaging, and to discuss future imaging applications.

Principle of adaptive optics

An adaptive optics system consists of two main optical components: a wavefront sensor to detect the shape of the wavefront generated by the eye's optics and a correcting element that dynamically compensates for the aberrations in the wavefront (see Fig. 1). Detailed reviews of adaptive optics are available elsewhere.^{14, 15} The most common wavefront sensor in vision science is the Shack-Hartmann type. This device samples the wavefront through an array of tiny lenslets. Each lenslet creates a focused spot, which is digitized by a CCD camera. The image, if representing a perfect, diffraction-limited wavefront, would be a uniform grid pattern. If, however, the wavefront has aberrations, the spots will not focus on-axis in the back focal plane of their corresponding lenslets but will deviate according to the slope of the wavefront at that lenslet. By use of a simple algorithm, the wave aberration can be constructed from the displacements of all the spots.

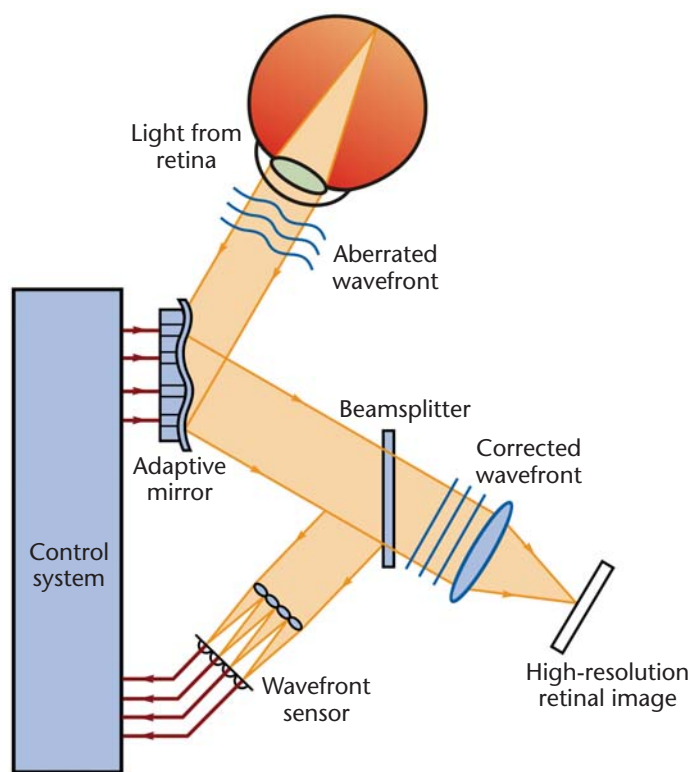


Figure 1. Schematic of an adaptive optics system. [Adapted from a figure by Chris Dainty, National University of Ireland, Galway.]

Once the wave aberration has been measured, it must be corrected. In vision science the most widely used correcting element is a deformable mirror. A deformable mirror consists of a flexible reflective layer supported from behind by an array of actuators (currently ranging from a few dozen to over 100 actuators) that deform the mirror to the desired shape. For "closed-loop" imaging systems, the wavefront sensor measures the wavefront, a computer calculates the required correction, and a signal is sent to the deformable mirror to generate the necessary shape to correct the wavefront aberrations. This measurement and correction cycle is repeated at a rate of 30 Hz until a certain threshold of correction is reached, at which point an image is taken.

Initial results for retinal imaging

Of the various cell types in the retina, scientists have focused on imaging the cone photoreceptors (although paradoxically, the cones make up only 5 percent of the total number of photoreceptors in the

retina). Many debilitating retinal diseases primarily affect the cones, and in normal vision, the cone mosaic places constraints on our spatial and color vision. The ability to visualize cones *in vivo* has thus been an attractive goal for many researchers. Like a tiny fiber optic, cones act as waveguides—collecting incoming light over some fixed acceptance angle and funneling the light along the length of the cone until it is reflected back through the cone [by the retinal pigment epithelium (RPE), the pigmented portion at the back of the eye] towards the pupil center. They can thus be seen even without complete correction of the eye's aberrations. As mentioned above, Miller et al. showed that correction of lower order aberrations enabled single cones to be visualized with a fundus imaging system, although only in eyes with excellent optical quality.⁸ But routine visualization of the cone photoreceptors only became possible with the advent of adaptive optics. Described below are some of the recent discoveries regarding the human visual system made possible by imaging

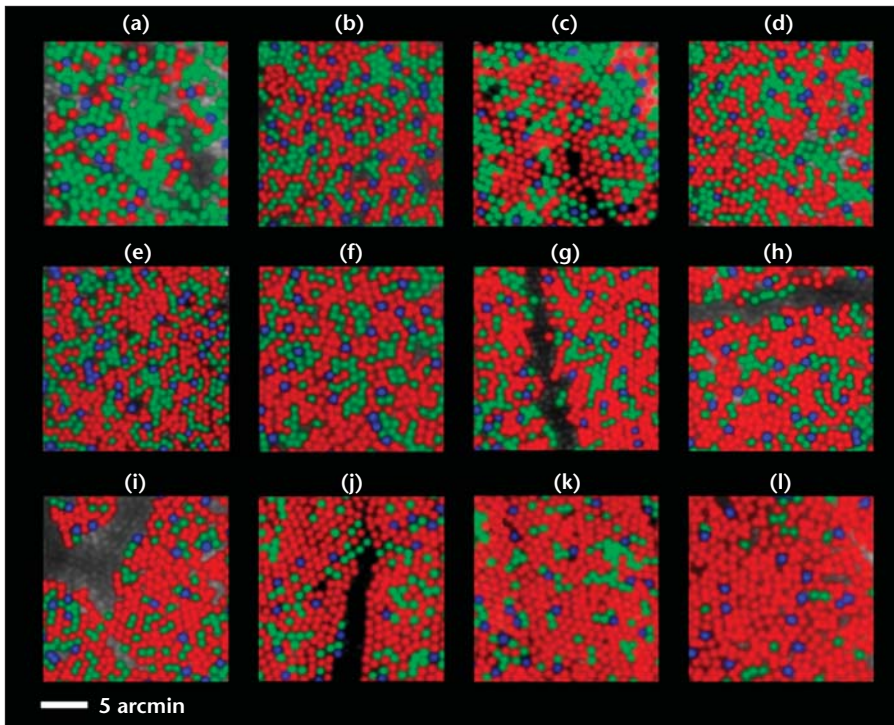


Figure 2. Pseudocolor images of the trichromatic cone mosaic. Images are from 10 different subjects (12 different retinal locations) and were obtained by combining adaptive optics imaging with retinal densitometry. Blue, green and red are used to represent the S, M and L cones, respectively. The L:M cone ratios are (a) 0.37, (b) 1.11, (c) 1.14, (d) 1.24, (e) 1.77, (f) 1.88, (g) 2.32, (h) 2.36, (i) 2.46, (j) 3.67, (k) 3.90, (l) 16.54. The proportion of S cones is relatively constant across eyes (3.9 – 6.6 percent of the total number of cones). Panels (d) and (e) show images from nasal and temporal retina in one subject, (j) and (k) show images from nasal and temporal retina in another subject. [Reproduced with permission from the MIT Press, Ref. 17.]

the cone mosaic with adaptive optics. The results described were obtained by use of conventional flood-illuminated imaging, where a flash lamp is used to illuminate a small patch of retina and a CCD camera is used to record the high-resolution fundus image. Other imaging techniques that incorporate adaptive optics are discussed later.

Organization of the human trichromatic cone mosaic

Human color vision is derived from the presence of three different cone types in the retina: short- (S-), middle- (M-) and long-wavelength sensitive (L-). While this has been known for over 200 years, the precise topography of the different cone types within the retina has proven elusive. From indirect techniques and examination of donor retinal tissue, it was known that the S cones made up only about 5 percent of the total number of cones. The remaining cones are L and M, and it

had been suggested (again from indirect techniques) that the ratio of L to M cones might vary across individuals. By using a selective bleaching technique in combination with adaptive optics retinal imaging, Roorda and Williams were able to deduce the spectral identity (S, M or L) of individual cones in retinal images.¹⁶ Results from two individuals confirmed the idea of intersubject variability in the L:M ratio and also demonstrated that the L and M cones are randomly arranged. Hofer and colleagues extended this technique to study eight additional subjects and revealed more extensive variability,¹⁷ as shown in Fig. 2. Remarkably, despite the 40-fold variation in L:M cone ratio, all subjects demonstrated normal color discrimination.¹⁸ In fact, one subject (panel l, Fig. 2) had fewer M cones than S cones but had superior color discrimination! The ability to directly determine the organization of the three cone types in the living retina will no doubt help vision

scientists uncover the developmental mechanisms underlying this widespread variation and examine its consequences for color vision.

Reflectance properties of individual cone photoreceptors

As mentioned above, the waveguide properties of the cones make them easy to visualize in adaptive optics imaging. Using off-axis illumination, Roorda and Williams found that the cone photoreceptors demonstrate remarkable precision in the alignment of their optical axes, with cones pointing to an area of the pupil that is less than 0.15 mm.¹⁹

A curious feature observed in high-resolution retinal images of the cone mosaic is that there is variation in the reflectance between different cones. Moreover, there is temporal variation in the reflectance of individual cones on scales ranging from a few seconds to a few days.²⁰⁻²² In an effort to determine the cause of this spatiotemporal variability, Pallikaris et al. monitored cone images obtained with adaptive optics over a 24-hour period.²¹ They found that the spatial variation was not caused by changes in cone directionality (i.e., pointing direction) but was likely mediated by intrinsic changes within the cone or the cone-RPE interface. The authors proposed that at least some of the temporal variation might be related to the process of disc shedding of the outer segments of the cone. If this is true, it could provide a metric with which to monitor the health of individual cones in vivo, in that cones that are unhealthy may exhibit abnormal rates of disc shedding.

A new cause for color blindness

One form of color blindness, red-green dichromacy, results from the functional loss of the L or M cone class, but a central question has been whether individuals with this form of color blindness have lost one population of cones or whether they have normal numbers of cones filled with either of two instead of three pigments. Although evidence has accumulated in favor of the second hypothesis (that the photopigment of one cone class is replaced), the issue has not been resolved.

The genes that encode the L- and M-cone photopigments reside on the

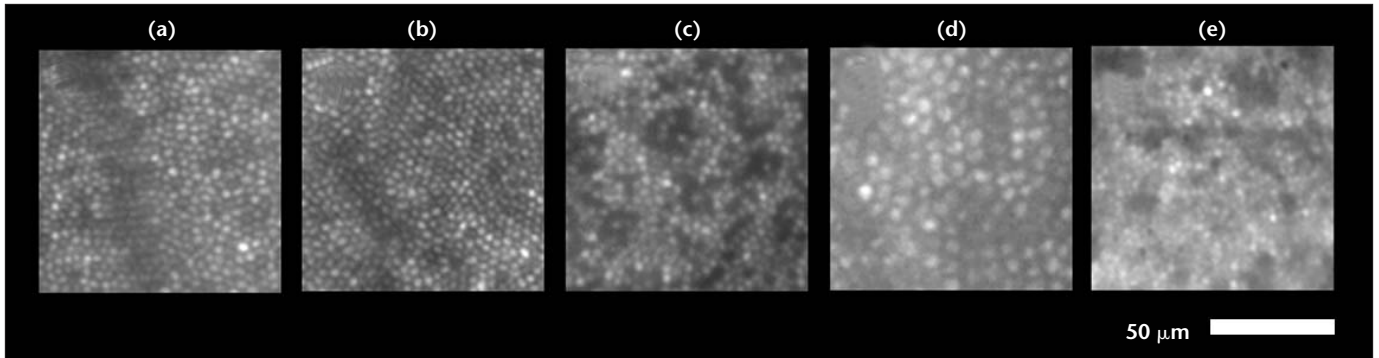


Figure 3. Imaging retinal disease with adaptive optics. (a-c) Images of the photoreceptor mosaic taken at approximately 1-degree eccentricity. (a) Subject JP, normal color vision. (b) Subject MM, red-green color vision deficient. All cones are of the S or M type, and cone density is similar to that of color normals. (c) Subject NC, red-green color vision deficient. All cones are of the S or L type and cone density is reduced by approximately 35 percent. The dark areas in the image are believed to be the location of M cones that have died or become severely malformed. (d and e) Images of the photoreceptor mosaic taken at approximately 4-degrees eccentricity. (d) Subject JP, normal color vision. (e) Subject RM, a congenital achromat. Achromatopsia is a disorder characterized by a complete loss of cone function and color perception. The photoreceptors in this image are probably rods, based on an analysis of their density and size for this retinal eccentricity. This result corroborates earlier histology results suggesting that achromats lack or have greatly reduced numbers of cone photoreceptors.

X chromosome. Two general categories of mutations of these genes have been found to be associated with red-green dichromacy. In one category, the gene(s) for one class of pigment have been deleted or replaced by a functional gene from a different class of pigment; in the other category, a normal gene is replaced by one encoding a photopigment that does not function properly. Using adaptive optics, retinal images were obtained from two individuals who represent the two different genetic categories of dichromat, to see if genetic variability would lead to phenotypic* variability in the cone mosaic.²³ One subject had a normal number of functional cones in the central retina, but his L-pigment gene had been replaced by one encoding a functional M photopigment; this meant, in effect, that his L cones had been replaced by M cones [Fig. 3(b)]. In an individual in whom the normal M-pigment gene was replaced by a gene that encodes a nonfunctional M pigment, patchy loss of normal cones throughout the photoreceptor mosaic was observed [Fig. 3(c)]. In this person, color blindness is associated with a normal mosaic of L and S cones, with interspersed dark patches where his normal M cones would have been. Remarkably, a loss of one-third of the cones in this subject impairs

only his color vision. These findings illustrate the usefulness of adaptive optics in uncovering genotype*-phenotype relationships that were previously difficult (or impossible) to study.

Uncovering details of retinal disease

Although our understanding of the genetic basis of retinal disease is advancing at a rapid pace,²⁴ the physical manifestation of disease is often more difficult to assess. Most of what we do know about retinal disease has come from studying donor tissue, which obviates the possibility of studying visual function in the same patient. One of the more exciting applications of adaptive optics retinal imaging has been towards providing earlier detection and improved diagnosis of retinal diseases. While promising results have been obtained with conventional flood-illuminated adaptive optics systems [see Fig. 3(e)], the realization of adaptive optics imaging as a tool to study retinal disease will no doubt involve other imaging technologies.

Combining adaptive optics with other technologies

Scanning laser ophthalmoscopy

A scanning laser ophthalmoscope (SLO) creates an image of the retina by raster scanning a laser beam into the eye and detecting the reflected light point by

point.²⁵ The main advantage afforded by the SLO over traditional imaging is improved efficiency in light collection (through the use of more sensitive detectors) and video-rate imaging capabilities. Additional benefit is obtained when confocal detection is implemented.²⁶ The benefit of confocal detection is two-fold: resulting images have higher contrast, and through axial scanning of the focal spot, axial slices of the retina can be obtained with ~300 nm resolution.²⁷

Confocal SLOs, which have been commercially available for over 15 years, have been an important tool for studying the coarse features of retinal disease. Some groups have used confocal SLOs to obtain retinal images in which information about the photoreceptor mosaic could be obtained through extensive image processing.^{20, 28} The implementation of adaptive optics to correct the eye's monochromatic aberrations further increases the lateral and axial resolution of a confocal SLO. Early efforts to correct lower order aberrations or statically correct higher order aberrations in combination with an SLO yielded only modest improvements in axial resolution and image contrast.^{7, 29} Recent integration of a real-time adaptive optics system (that corrects the higher order aberrations of the eye) with an SLO by Roorda et al. enabled the first high-resolution SLO images of the retina,³⁰ in which axial sectioning (see Fig. 4) is greatly improved

* Phenotype - The physical appearance/observable characteristics of an organism.

* Genotype - The genetic constitution of an organism.

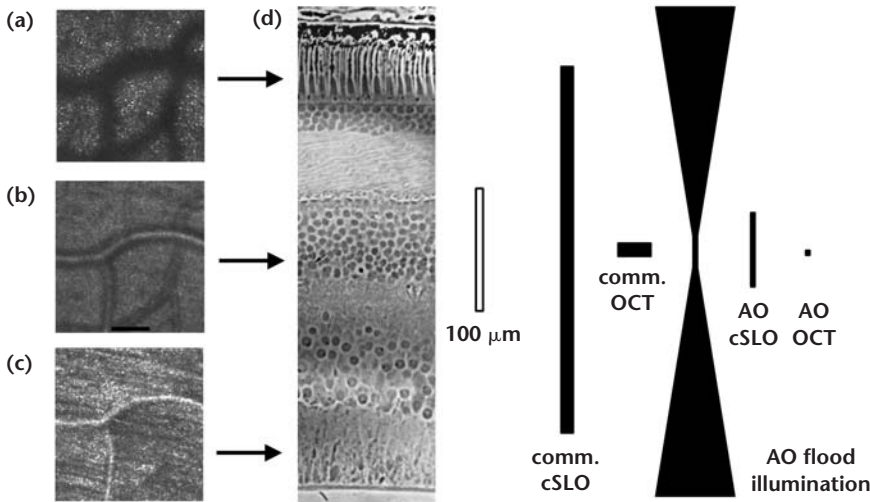


Figure 4. Axial sectioning of the human retina and resolution of current imaging devices. On the left are images from a confocal AOSLO focused at the photoreceptor layer (a), the inner nuclear layer (b) and the nerve fiber layer (c). The blood vessel appears dark in (a) because scattered light from its surface is blocked by the confocal pinhole. The scale bar in (b) is 100 μm , and is the same for all three retinal images. (d) Histological cross section of the human retina; from Ref. 52, reproduced with permission from the Royal Society of London. On the far right are theoretical point-spread functions (PSF) for various combinations of AO and camera architectures (cSLO, OCT, and conventional flood illumination). For simplicity the PSFs are displayed as 2D projections with their width and height representing lateral and axial resolution, respectively. Note that the displayed PSF for the AO flood illuminated camera represents an effective PSF rather than the true PSF, i.e., the out of focus light from other planes only contributes to a loss of contrast, not resolution. Two commercial cameras (comm. cSLO and comm. OCT) are also shown. [PSF analysis courtesy of Don Miller, Indiana University.]

($\sim 100 \mu\text{m}$ axial resolution) and cells as small as $3 \mu\text{m}$ can be readily visualized. Shown in Fig. 5 is an image of white blood cell flow through parafoveal capillaries, deduced from an analysis of successive video frames.

Optical coherence tomography (OCT)

Of all the ophthalmic imaging devices, OCT is perhaps the most rapidly developing.³¹ A number of commercially available instruments are already in clinical use and serve as an invaluable tool for clinicians in diagnosing retinal disease.³² Many groups are working to improve the clinical utility of future devices by improving their speed, sensitivity and resolution. The main advantage of OCT is that it provides good depth resolution, allowing clinicians to visualize different retinal layers [depicted in Fig. 4(d)]. But commercial OCT systems have approximately $25 \mu\text{m}$ lateral and $10 \mu\text{m}$ axial resolution, a level that is too poor to resolve any cellular structures in the retina. Recently however, researchers from the University

of Vienna and the University of Murcia have combined an ultrahigh-resolution OCT system (using ultrabroad-bandwidth light sources) with a closed-loop adaptive optics system.³³ They improved the resolution with this AO-OCT instrument to about $5\text{-}10 \mu\text{m}$ lateral and $3 \mu\text{m}$ axial resolution, with the main benefit so far being an increase in the number of photons captured by the detector. Images from this system are shown in Fig. 6. Further improvement of the adaptive optics system could enable three-dimensional visualization of photoreceptors, ganglion cells or capillaries in the retina (see Fig. 4). Just how successful this effort will ultimately be depends on a number of factors, including the contrast of the retinal structures of interest, whether adequate photons can be collected to obtain useful images and improvements in methods to avoid image artifacts caused by eye motion.

Image processing

The high cost and large size of the first adaptive optics systems were seen by

many vision scientists as prohibitive. An alternative to *optical* correction of the eye's aberrations is to *computationally* correct them using deconvolution. This approach has not yielded retinal images with the resolution required to resolve individual cells.^{34,35} However, a theoretical analysis showed that a hybrid technique using *both* adaptive optics imaging and deconvolution could give an improved signal-to-noise ratio over deconvolution alone³⁶; this result is not surprising since the approach has been used successfully in astronomical applications. Moreover, Christou et al.³⁷ found that deconvolving high resolution images obtained with adaptive optics improves the contrast of the images by a factor of 6, makes individual cones easier to identify (via a reduction of the full-width-half-max of each cone by a factor of 3) and improves the ability to classify cones as S, M or L using the selective bleaching paradigm discussed previously. Christou has applied deconvolution to retinal images obtained with adaptive optics by Choi and colleagues, which increases the visibility of rod photoreceptors that are otherwise difficult to resolve.³⁸

Other image processing techniques have demonstrated important utility for vision scientists. Montaging methods that take individual retinal images (each approximately 1 degree field of view) and create a wide-field (~ 4 degrees), high-resolution image allow researchers to obtain a larger view of the retina³⁹ and to more easily quantify retinal features across the retina.²³ In addition, while individual retinal images are of good resolution, significant cone contrast improvements are obtained by averaging together many images of the same area of retina. Lastly, in scanning systems, eye movements and scanner nonlinearities cause image distortions that prevent the averaging of images through simple shift-and-add methods.⁴⁰ Algorithms are currently under development to measure and remove these distortions.

Future directions for adaptive optics systems

Towards a clinical system

While the majority of the results reviewed in this article used a conventional

continuous face-plate deformable mirror to perform the wavefront correction, there are a number of other corrective elements that can be used to optically compensate for the aberrations inherent in a particular wavefront. The primary appeal of these devices is lower cost, a feature that will become even more relevant as clinical systems are designed. In addition, they are typically smaller and more compact, with a corresponding reduction in overall system size. Devices that have resulted in high-resolution retinal images (comparable to those obtained with the conventional continuous face-plate deformable mirror) include a bimorph curvature mirror,^{39,41} an electrode-driven membrane mirror,¹³ a liquid-crystal spatial light modulator⁴² and a microelectromechanical (MEMS) mirror.⁴³

In addition to the use of alternate corrective elements, advances in wavefront sensing will help bring the cost of adaptive optics retinal imaging down and at the same time increase the accuracy of the wavefront correction. Other improvements will certainly include retinal and pupil tracking for image stabilization and enhanced post-processing algorithms. Together, these improvements are a key step towards ultimately delivering a clinical instrument that can be used for earlier detection and better diagnosis of retinal diseases. In addition, they will enable wider dissemination of adaptive optics imaging systems to basic scientists.

These new systems are not as far off as one might think. Currently, the Center for Adaptive Optics (CfAO),* a National Science Foundation Science and Technology Center, brings together researchers from 11 universities and 11 industrial associates in order to develop next generation adaptive optics systems and to optimize current systems. Two Bioengineering Research Partnerships (BRP) funded by the National Eye Institute, one led by David Williams at the Institute of Optics at Rochester and another by Jack Werner at the University of California, Davis, have stemmed from CfAO activities. One group will design and build six new adaptive optics systems for high-resolution retinal imaging (doubling the

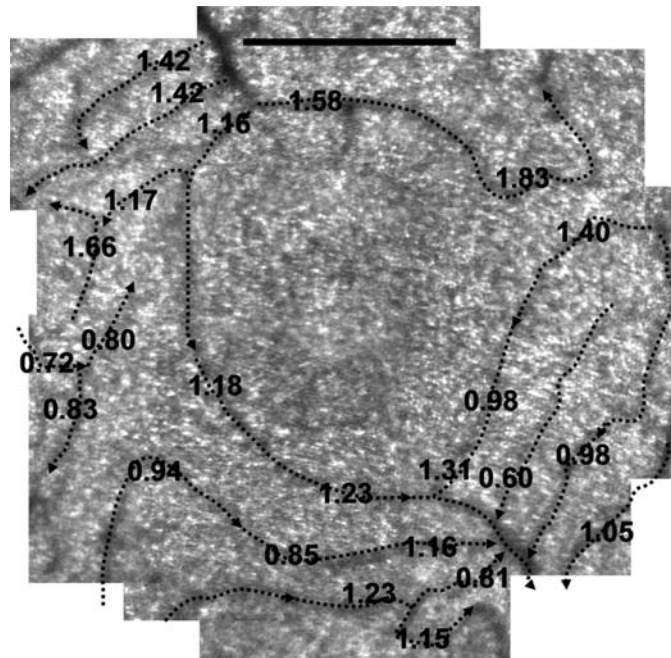


Figure 5. Composite image of the parafoveal capillary network of a single subject taken with the adaptive optics scanning laser ophthalmoscope. The image was stitched together from frames extracted from a series of parafoveal video sequences. The overlay shows the velocity of the observed leukocytes in mm/s in each capillary. The dashed lines indicate the direction of flow in each capillary. The scale bar at the top of the image spans 1 degree of visual angle, which is about 300 μm . [Image courtesy of Joy Martin, University of Houston.]

number of systems in operation in the United States); the other group will work on developing integrated AO-OCT systems. In Europe, there are similar consortia—the SHARP-EYE network* and the Smart Optics Faraday Partnership**—which also have the goal of developing new and improved retinal imaging adaptive optics systems.

Beyond imaging cones ...

Numerous groups have demonstrated that cone photoreceptors can be easily visualized using adaptive optics imaging systems.^{11, 30, 39, 42, 44, 45} Many retinal diseases are characterized by photoreceptor degeneration, so current imaging technology may be sufficient to allow adaptive optics to play a major role in the improved detection and diagnosis of such diseases. But other debilitating retinal diseases, such as glaucoma and age-related macular degeneration (AMD), affect other cell types (ganglion cells and RPE cells, respectively). Recent findings

provide hope that these cell types can also be imaged *in vivo*, resulting in earlier detection of these diseases and more effective treatment.

With the photoreceptors residing at the back of the retina, incident light must pass through all the other cell types (e.g., ganglion cells) before being detected. Fortunately for our vision (though unfortunately for imaging) these cells are generally transparent. One approach that has already demonstrated enhanced capability to image non-photoreceptor cell types is fluorescence imaging. Dacey et al. injected a retrograde label (rhodamine dextran) into the lateral geniculate nucleus (LGN) and imaged ganglion cells *ex vivo* using a standard confocal microscope.⁴⁶ Using a confocal SLO, Fitzke and colleagues obtained images of ganglion cells in living rat and primate retinae.⁴⁷ They used an intravitreal injection of an Annexin 5-bound fluorophore that only becomes active when a cell is undergoing cell death. Thus they were able to track in real-time individual ganglion cells that were dying as a result

* <http://cfao.ucolick.org/>.

* <http://www.sharpeye.org/>.

** <http://www.smartoptics.org/>.

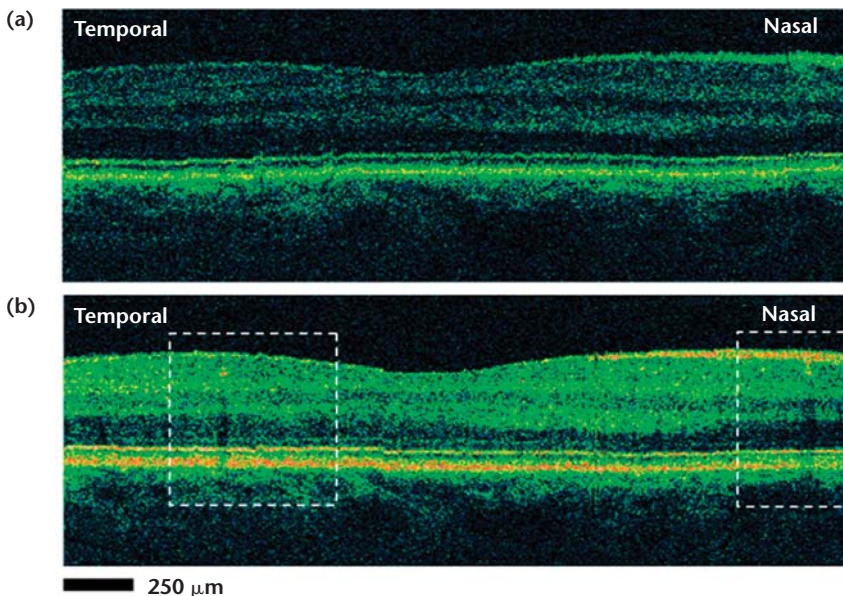


Figure 6. In vivo OCT tomograms without (a) and with (b) adaptive optics. The use of adaptive optics increases the transverse resolution of the OCT image to 5-10 μm , and improves the signal to noise ratio by up to 9 dB. [Reproduced with permission from OSA, Ref. 33.]

of experimentally induced cell death. This approach will prove useful to the understanding of the progression of glaucoma, especially in animal models of the disease. The key to human imaging will be delivery of contrast enhancing agents so that with the appropriate laser source and filter set, cells that were otherwise invisible in reflectance imaging can be imaged noninvasively.

RPE cells exhibit autofluorescence; the signal results from the presence of lipofuscin. With confocal SLOs, it is possible to image the RPE cell layer in vivo without injecting any dyes or labels.⁴⁸ RPE autofluorescence in humans has been extensively studied and elevated autofluorescence has been found to be associated with regions of atrophy in eyes with AMD.⁴⁹ Commercial confocal SLOs have been used to study changes in autofluorescence in retinal disease,⁵⁰ and the future application of AOSLO imaging to obtain high-resolution autofluorescence maps of the retina will help elucidate the role of increased autofluorescence in disease progression.

Lastly, vascular attenuation and changes in blood flow are hallmarks of many retinal diseases. While it has been possible to image blood flow using commercial SLO systems in combination with

intravenous injection of fluorescent dyes, such measurements have been largely limited to animal studies.⁵¹ The recent measurements (see Fig. 5) made with the AOSLO provide an attractive, noninvasive alternative for studying blood flow dynamics in vivo and will serve as a stepping-stone for future work in studying diseased eyes. The fact that adaptive optics is compatible with so many other methods to enhance retinal imaging opens many new doors for future research. The most exciting applications of adaptive optics for retinal imaging are probably yet to come.

Acknowledgments

The authors thank Pablo Artal, Li Chen, Stacey Choi, Chris Dainty, Nathan Doble, Wolfgang Drexler, Julianna Lin, Joy Martin, Don Miller, Jason Porter, Jack Werner and Jessica Wolfing for helpful discussion and assistance.

Joseph Carroll (jcarroll@cvs.rochester.edu) is a post-doctoral fellow in the Center for Visual Science at the University of Rochester. **Daniel C. Gray** is a graduate student in the Institute of Optics at the University of Rochester.

David Williams is the William G. Allyn Chair of Medical Optics, director of the Center for Visual Science and a professor of Brain and Cognitive Sciences at the University of Rochester. **Austin Roorda** is a professor in the School of Optometry at the University of California, Berkeley.

References

1. H. W. Babcock, *Publ. Astron. Soc. Pac.* **65**, 229-36 (1953).
2. A. Greenaway and J. Burnett, *Industrial and Medical Applications of Adaptive Optics*, IOP Publishing Ltd., Bristol, U.K. (2004).
3. Z. Kam et al., *Proc. Natl. Acad. Sci. USA* **98**, 3790-5 (2001).
4. M. J. Booth et al., *Proc. Natl. Acad. Sci. USA* **99**, 5788-92 (2002).
5. M. S. Smirnov, *Biophysics* **6**, 766-95 (1961).
6. P. Artal and R. Navarro, *Opt. Lett.* **14**, 1098-100 (1989).
7. A. W. Dreher et al., *Appl. Opt.* **28**, 804-8 (1989).
8. D. T. Miller et al., *Vision Res.* **36**, 1067-79 (1996).
9. J. Liang et al., *J. Opt. Soc. Am. A Opt. Image Sci. Vis.* **11**, 1949-57 (1994).
10. J. Liang and D. R. Williams, *J. Opt. Soc. Am. A Opt. Image Sci. Vis.* **14**, 2873-83 (1997).
11. J. Liang et al., *J. Opt. Soc. Am. A Opt. Image Sci. Vis.* **14**, 2882-92 (1997).
12. H. Hofer et al., *J. Opt. Soc. Am. A Opt. Image Sci. Vis.* **18**, 497-506 (2001).
13. E. J. Fernandez et al., *Opt. Lett.* **26**, 746-8 (2001).
14. R. K. Tyson, *Principles of Adaptive Optics*, Academic Press Inc., San Diego (1991).
15. J. Porter et al. eds., *Adaptive Optics for Vision Science: Principles, Practices, Design, and Applications*, Wiley & Sons Inc. (in press, see <http://cfao.uclick.org/> for updates).
16. A. Roorda and D. R. Williams, *Nature* **397**, 520-2 (1999).
17. D. R. Williams and H. Hofer, *The Visual Neurosciences*, L.M. Chalupa and J.S. Werner, eds., MIT Press, Cambridge, Mass., 795-810 (2004).
18. J. Neitz et al., *Neuron* **35**, 783-92 (2002).
19. A. Roorda and D. R. Williams, *J. Vis.* **2**, 404-12 (2002).
20. A. R. Wade and F. W. Fitzke, *Lasers and Light in Ophthalmology*, **8**, 129-36 (1998).
21. A. Pallikaris et al., *Invest. Ophthalmol. Vis. Sci.* **44**, 4580-92 (2003).
22. J. Rha et al., presented at Frontiers in Optics, the 88th OSA Annual Meeting, Rochester, N.Y., 2004 (unpublished).
23. J. Carroll et al., *Proc. Natl. Acad. Sci. USA* **101**, 8461-6 (2004).
24. A. Rattner et al., *Annu. Rev. Genet.* **33**, 89-131 (1999).
25. R. H. Webb and G. W. Hughes, *IEEE Trans. Biomed. Eng.* **28**, 488-92 (1981).
26. R. H. Webb et al., *Appl. Opt.* **26**, 1492-9 (1987).
27. R. Birngruber et al., *Graefes Arch. Clin. Ex. Ophthalmol.* **238**, 559-65 (2000).
28. A. Roorda and M. C. W. Campbell, in *Vision Science and Its Applications Technical Digest Series*, Vol. 1 (Optical Society of America, Washington, D.C., 1997), pp. 90-3.
29. S. A. Burns et al., *Opt. Lett.* **27**, 400-2 (2002).
30. A. Roorda et al., *Opt. Express* **10**, 405-12 (2002).
31. R. D. Ferguson et al., *Opt. Lett.* **29**, 2139-41 (2004).
32. P. Hrynchak and T. Simpson, *Optom. Vis. Sci.* **77**, 347-56 (2000).
33. B. Hermann et al., *Opt. Lett.* **29**, 2142-4 (2004).
34. I. Iglesias and P. Artal, *Opt. Lett.* **25**, 1804-6 (2000).
35. D. Catlin and C. Dainty, *J. Opt. Soc. Am. A Opt. Image Sci. Vis.* **19**, 1515-23 (2002).
36. J. Arines and S. Bara, *Opt. Express* **11**, 761-6 (2003).
37. J. C. Christou et al., *J. Opt. Soc. Am. A Opt. Image Sci. Vis.* **21**, 1393-401 (2004).
38. S. S. Choi et al., *Invest. Ophthalmol. Vis. Sci.* **45**, E-Abstract 2794 (2004).
39. M. Glanc et al., *Opt. Commun.* **230**, 225-38 (2004).
40. M. Stetter et al., *Vision Res.* **36**, 1987-94 (1996).
41. J.-F. Le Gargasson et al., *C. R. Acad. Sci., Paris II*, 1131-8 (2001).
42. F. Vargas-Martin et al., *J. Opt. Soc. Am. A Opt. Image Sci. Vis.* **15**, 2552-62 (1998).
43. N. Doble et al., *Opt. Lett.* **27**, 1537-9 (2002).
44. N. Ling et al., *High-Resolution Wavefront Control: Methods, Devices, and Applications IV, Proceedings of the SPIE*, Vol. 4825, J.D. Gonglewski et al., eds., 99-108 (2002).
45. N. Ling et al., presented at Frontiers in Optics, the 88th OSA Annual Meeting, Rochester, N.Y., 2004 (unpublished).
46. D. M. Dacey et al., *Neuron* **37**, 15-27 (2003).
47. M. F. Cardeiro et al., *Proc. Natl. Acad. Sci. USA* **101**, 13352-6 (2004).
48. A. von Ruckmann et al., *Br. J. Ophthalmol.* **79**, 407-12 (1995).
49. F. G. Holz et al., *Graefes Arch. Clin. Ex. Ophthalmol.* **237**, 145-52 (1999).
50. N. Lois et al., *Br. J. Ophthalmol.* **84**, 741-5 (2000).
51. P. F. Sharp et al., *Phys. Med. Biol.* **49**, 1085-96 (2004).
52. B. B. Boycott and J. E. Dowling, *Philos. Trans. R. Soc. Lond., B, Biol. Sci.* **255**, 109-94 (1969).